JOURNAL OF MATERIALS SCIENCE 30 (1995) 693–700

Multiparticle clusters and carbon superstructure in martensite

L. DABROWSKI
Institute of Atomic Energy, 05-400 Otwock-Swierk Poland

On the basis of experimentally verified concentration expansion tensor values, stress induced two-particle C–C potentials have been calculated in harmonic approximation. A calculation method has been developed and expressions derived for the evaluation of multiparticle interaction potentials and cluster population. The temperature range of the applicability of the method has been estimated. On the basis of this method it has been demonstrated that in thermodynamic quasi-equilibrium, carbon atoms exist in clustered form. The clusters most frequently appearing at 300 K are of four- and five-particle type. The cluster configurations have been determined and the binding energy per atom has been estimated as about 0.5 eV. At 78 K, there exist practically only five-particle linear clusters situated along the tetragonal C axis. It has been postulated that a superstructure may exist in martensite with a binding energy per atom nearly four times higher than in the case of the above clusters. The presence of superstructure is associated with the formation of five-atom seeds in the form of pyramids having their basis in the (0 0 1) plane. The formation of seeds with different topology from the other clusters is associated with overcoming a potential barrier. The postulated form of ordering at low temperatures should exhibit high thermal stability with respect to ordering changes and order–disorder phase transitions, as well as to carbide formation.

1. Introduction

In the structure of martensite, an interstitial solid solution, carbon occupies octahedral sites with preference to occupying O_c-site positions [1, 2]. Theoretical calculations demonstrate that the tetrahedral sites can be occupied only temporarily during diffusion of carbon atoms from one octahedral position to another [3]. Many years of systematic investigation of short range order by Mössbauer effect (ME) and nuclear magnetic resonance (NMR) spectroscopy methods (cf. a review paper by Genin [4]) have revealed distinct statistical deviations of carbon distribution in the solution. Thus, for instance, in freshly quenched martensite with a carbon content of 9.5 at.%, practically all carbon atoms exist in isolated form. After ageing at room temperature the number of isolated carbon atoms drops as a result of diffusion, and stabilizes in the course of 12 days at a level of about 20% [4]. There is no doubt that carbon clusters have been formed in this case.

Although the problem of specific forms of short-range carbon configuration has been attracting attention for many years, it has never been satisfactorily solved. The resolution of experimental methods is too low to allow for an unambiguous interpretation, and the results of theoretical analysis have not been sufficiently complete thus far. Nevertheless, valuable information has been obtained on theoretical grounds [3, 5, 6]. Some two-particle C–C stress induced potentials in body centred tetragonal (bct) martensite structure have been estimated under the assumption that carbon occupies octahedral sites. It follows from these calculations that for some pairs, such as C–C$\frac{1}{2}\langle 1\,1\,1\rangle$, C–C $\langle 1\,1\,0\rangle$ or C–C $\langle 1\,0\,0\rangle$, these potentials are negative and of significant magnitude (0.13–0.44 eV). As a consequence, preferential formation of such clusters may occur. In a previous paper [7], numerical estimation of the probability of the existence of a given cluster has been made. It follows from these calculations that strong correlations exist in this system as regards occupation of interstitial sites, leading to major modifications in the distribution of carbon atom pairs with respect to statistical distribution.

As it follows from [5, 6], stress induced potentials in carbon martensite extend over long distances. The authors of the above references calculated these potentials in a volume comprising 26 co-ordination shells. It cannot be excluded that non-negligible interactions may extend over much greater distances in some crystallographic directions. This may have a profound effect on both: a possibility of the existence of multiparticle carbon clusters and their formation dynamics. The above theoretical reasoning justifies an assumption that much larger clusters may form in this system, as evidenced by some experimental investigations. Thus for example in [4], some satellite Mössbauer lines are interpreted as generated by a three-particle cluster with distances a–$b\frac{1}{2}\langle 1\,1\,1\rangle$, b–$c\frac{1}{2}\langle 1\,1\,1\rangle$ and a–$c\langle 1\,1\,0\rangle$.

The main task of the present paper is to identify the most probable two-particle clusters and to examine

0022–2461

possibilities of their growth into multiparticle clusters, as well as the possibilities of forming long range carbon configurations, i.e. superstructure formation.

2. Stress induced interaction

Ordering in interstitial solid solutions can be described on the basis of theoretical methods developed for substitutional alloys. Therefore, the Hamiltonian of the system, given in [8] can be written for the considered case in the form

$$\hat{H} = \hat{H}_0 + \sum_i V_i \hat{C}_i + \frac{1}{2}\sum_{ij} V_{ij}\hat{C}_i\hat{C}_j + \ldots + \frac{1}{n}\sum_{ij\ldots k} V_{ij\ldots k}\hat{C}_i\hat{C}_j\ldots\hat{C}_k \quad (1)$$

Where $\hat{H}_0$ is the Hamiltonian of pure iron matrix: V_i, $V_{ij}\ldots V_{ij\ldots k}$, the irreducible potentials of one-, two-, and n-particle C–C interactions, respectively, (the suffixes $ij\ldots k$ label the carbon lattice positions); $\hat{C}_i(\hat{C}_j\ldots\hat{C}_k)$ the local carbon concentration operators in $i(j\ldots k)$ positions, which are random functions equal to one, when position $i(j\ldots k)$ is occupied by a carbon atom or zero in other cases.

The first two terms in Hamiltonian Equation 1 induce a constant free energy shift independent of the degree of short and long range order, and may be omitted. The problem of calculating further terms of the expansion series, Equation 1, has been solved thus far only in harmonic approximation [6, 9–13]. This approximation makes it possible to calculate only two-particle potentials, V_{ij}, and, consequently the series has to be cut-off at the third term.

To calculate potentials V_{ij}, it is necessary to know the Born-von-Karmann elastic constants and components of concentration expansion tensor for the matrix material, being pure α-Fe in our case. The material constants obtained experimentally by various authors differ substantially between each other. Table I presents elastic constants of α-Fe, obtained in [14–16]. As may be seen, all values bear a significant measurement error and for some of them, β_4, β_5, there is even disagreement in the sign of the reported values.

Further errors in calculation of V_{ij} result from discrepancies in the determination of the values of concentration expansion tensor. They can be calculated on the basis of the measurement of martensite lattice constants a and c. However, their values depend, among others, on the degree of alloy ordering; thus introducing an interpretation ambiguity. The above situation calls for a more detailed discussion.

Under the assumption that carbon atoms occupy octahedral lattice sites, the components of the concentration expansion tensor are associated with the martensite lattice parameters by the following relations [5]

$$\begin{aligned} a &= b = a_0[1 + \alpha n/3 - \beta n\eta/3] \\ c &= a_0[1 + \alpha n/3 + 2\beta n\eta/3] \end{aligned} \quad (2)$$

Where a, b, c are lattice parameters of martensite; a_0 is the lattice parameter of α-Fe; n the atomic concentration of carbon; η the long range order parameter; α equal $2U_{11} + U_{33}$: β, equal $U_{33}-U_{11}$; and U_{11} and U_{33} are components of the concentration expansion tensor.

Parameter η is associated with the mean carbon concentration in sublattices O_a, O_b, and O_c as follows

$$\begin{aligned} n(O_a) &= n(O_b) = n(1-\eta)/3 \\ n(O_c) &= n(1+2\eta)/3 \end{aligned} \quad (3)$$

It follows from Equations 2 and 3 that parameter η is defined in such a way that if η = 1, carbon occupies only O_c lattice sites. The lattice tetragonality is at its maximum in this case. If η = O, the tetragonal lattice transforms into a cubic one, and the carbon concentrations in all sublattices are identical.

By solving Equation 2 with respect to parameters α and β

$$\begin{aligned} \alpha &= 2(a/a_0 - 1)/n + (c/a_0 - 1)/n \\ \beta &= (c/a_0 - a/a_0)/(n\eta) \end{aligned} \quad (4)$$

It follows from Equation 4, coefficient β, unlike α, can be determined only when the long-range order parameter, η, is known.

Under the assumption that η = 1, and on the basis of empirical dependencies of martensite lattice constants a and c on concentration, [5] determined the values of α and β as 0.66 and 0.96, respectively. On the other hand, I.R. Entin *et al.* [2] demonstrated experimentally that in freshly quenched martensite of normal tetragonality η = 0.7. The experiment was conducted by means of neutron diffraction on Fe–Ni–C alloy of specially prepared isotope composition, and the result was obtained on the basis of carbon reflections (the matrix reflections were eliminated).

If one assumes that η = 0.7, then α = 0.66 and β = 1.37. Kurdiumov *et al.* [5] performed calculations of V_{ij} for both situations. The obtained results differ substantially between each other. By making use of the V_{ij} values obtained by Kurdiumov *et al.*, [5] one can calculate temperature dependencies, $\eta(T)$, for both situations [7]. It appears that there are almost three-fold differences in the temperatures of order–disorder phase transitions. Thus, knowledge of the degree of ordering is of essential importance.

Measurements of η by neutron diffraction, such as those performed in [2], bear unfortunately significant

TABLE I Born-von-Karmann elastic constants for α-Fe × 10^4 dyn cm^{-1}. The notation follows [17].

Ref	α_1	α_2	α_3	$-\alpha_4$	$-\alpha_5$	β_1	β_2	$-\beta_3$	β_4	β_5	γ_3	γ_4	δ_4
14	1.688	1.463	0.092	0.012	0.029	1.501	0.055	0.057	0.003	0.032	0.069	0.052	0.0007
15	1.628	1.552	0.118	0.023	0.046	1.485	0.054	0.088	0.024	−0.030	0.127	0.039	0.0070
16	1.786	1.492	0.124	0.060	0.023	1.491	0.036	0.109	−0.006	−0.024	0.030	0.028	0.0100

errors. It seems more reasonable to measure martensite parameters a and c as functions of temperature. Freshly quenched martensite of normal tetragonality exhibits a weak temperature dependence in the range 4.2–300 K [18, 19]. This is probably associated with formation of stable short range configurations comprising carbon atoms in sublattices O_a and O_b, which prevent carbon migration to sublattice O_c. On the other hand, the temperature dependence of c/a in martensite of anomalous tetragonality, reported in the above cited references is well marked and its course resembles relation $\eta(T)$ calculated in [7] ($c/a \sim \beta n \eta$ [5]). By extrapolating relations $a(T)$ and $c(T)$ for martensite of anomalous tetragonality to O K, one obtains the lattice parameters for $\eta = 1$. There exists an additional problem. Hamiltonian Equation 1 is expanded around $\hat{H}_0$ of pure α-Fe and, consequently, all material constants refer to α-Fe. It is known that the volume of quenching induced martensite is greater than that of austenite, and as a result an isotropic compressive stress, absent in pure iron, exists in the material. In view of Equation 4, one can see that these stresses are a source of systematic error, which leads to underestimation of the values of α and β obtained. The experimental data presented in [18] lead to $\alpha = 0.76$, while those from [19], to $\alpha = 0.57$. On the other hand, in [5] it is assumed that $\alpha = 0.66$. Since this parameter is independent of the degree of alloy ordering, its value should be independent of the method of sample preparation. Such significant differences cannot be explained by measurement errors (the resolution of the X-ray spectrometer was about 0.0002 nm). All the above mentioned examples refer to samples of bulk materials with significant internal stress.

To diminish such effects a series of X-ray diffraction measurements were performed as functions of temperature, using thin (30 μm) martensite foils of relatively low carbon content (4 at %C), quenched in liquid nitrogen (retained austenite content, 2.8%). The measurements gave an α value of 1.02 [20]. On the basis of extrapolation of temperature dependencies of lattice parameters to 0 K $\beta = 1.845$ was obtained, which leads to $U_{11} = -0.275$ and $U_{33} = 1.57$; an error was estimated, as $\Delta U_{11} = \pm 0.02$ and $\Delta U_{33} = \pm 0.08$.

Using the concentration expansion constants determined in this way, V_{ij} values were calculated by the pseudopotential method described in [6, 9–13]. Into account were taken 266 thousands of momentum vectors, k, from the first Brillouin zone. The calculations were performed in three versions, each making use of various sets of elastic constants presented in Table I. The results of the calculations are summarized in Table II, columns 3–5, in order of descending $|V_{ij}|$. values. Column 6 presents the values of the same potentials averaged over the three versions. Table II presents only the potentials with absolute values greater than 0.025 85 eV (i.e. corresponding to 300 K). The last column also presents the averaged potential values calculated at extreme values of the concentration expansion tensor, $U_{11}^* = U_{11} - \Delta U_{11} = -0.295$ and $U_{33}^* = U_{33} + \Delta U_{33} = 1.65$. It follows from the data presented in Table II that errors in determination of elastic constants do not affect the sequence and the

TABLE II The values of stress induced energies, $V(x, y, z)$ of the C–C pairs interaction (in eV) between a carbon atom located at the hkl position and another carbon atom located at the 0 0 0 position of the O_c sublattice. The values of potentials in columns 3, 4 and 5 are calculated on the basis of elastic constants from [14]–[16], respectively. Column 6 presents mean values of potentials. All potentials are calculated for values $U_{11} = -0.275$ and $U_{33} = 1.57$. Column 7 shows mean values of these potentials calculated for extreme values $U_{11}^* = -0.295$ and $U_{33}^* = 1.65$

No.	h	K	l	V_{ij} [14]	V_{ij} [15]	V_{ij} [16]	$\langle V_{ij} \rangle$	$\langle V_{ij}^* \rangle$
1	2			3	4	5	6	7
1	0	0	1	4.760 27	4.722 10	4.659 660	4.714 01	5.159 80
2	0	0	2	− 0.722 70	− 0.725 23	− 0.714 950	− 0.720 96	− 0.790 05
3	1/2	1/2	3/2	0.463 62	0.428 78	0.459 857	0.450 75	0.495 15
4	1/2	1/2	1/2	− 0.380 99	− 0.349 41	− 0.372 900	− 0.367 77	− 0.403 91
5	1	0	0	− 0.228 36	− 0.182 32	− 0.186 760	− 0.199 15	− 0.219 43
6	0	1	2	0.119 99	0.109 52	0.118 990	0.116 17	0.127 68
7	1	1	2	0.070 79	0.058 69	0.071 490	0.066 99	0.074 43
8	1/2	0	1	− 0.057 93	− 0.057 25	− 0.056 460	− 0.057 21	− 0.062 63
9	3/2	0	1	− 0.057 93	− 0.057 25	− 0.056 460	− 0.057 21	− 0.062 63
10	0	0	6	0.057 50	0.057 05	0.056 220	0.056 92	0.062 26
11	0	0	5	0.055 59	0.055 47	0.054 570	0.055 91	0.060 36
12	1/2	1/2	5/2	− 0.051 07	− 0.052 60	− 0.060 080	0.054 58	− 0.059 90
13	1	1	0	− 0.070 12	− 0.055 33	− 0.035 320	− 0.053 59	− 0.057 31
14	0	0	4	0.045 97	0.046 70	0.046 240	0.046 30	0.050 51
15	2	0	0	− 0.043 48	− 0.044 57	− 0.046 210	− 0.044 75	− 0.048 71
16	3/2	1/2	1/2	− 0.048 92	− 0.043 70	− 0.039 830	− 0.044 15	− 0.048 15
17	2	0	1	0.037 97	0.042 86	0.044 600	0.041 81	0.045 60
18	1	0	1	0.052 65	0.037 33	0.032 150	0.040 71	0.044 90
19	5	0	0	− 0.040 40	− 0.038 93	− 0.038 790	− 0.039 37	− 0.043 11
20	0	1/2	0	0.040 15	0.038 82	0.038 600	0.039 19	0.042 91
21	4	0	0	− 0.039 15	− 0.038 31	− 0.038 570	− 0.038 68	− 0.042 34
22	3	0	0	− 0.035 54	− 0.036 78	− 0.038 280	− 0.036 87	− 0.040 31
23	3/2	1/2	5/2	0.037 61	0.032 36	0.035 560	0.035 17	0.038 78
24	1	1	1	− 0.025 21	− 0.021 24	− 0.041 550	− 0.029 34	− 0.034 02

signs of potentials. This indicates that the solution obtained at such values of constants U_{ij} is stable. A comparison of the obtained V_{ij} values with those reported in [3, 5, 6] shows a qualitative agreement. The results presented in Table II confirm the existence of all clusters predicted in these papers (the appropriate V_{ij} potentials are negative and large in magnitude). There is, however, an essential difference. It follows from the data in Table II (column 6, line 2) that it should be the C–C $\langle 0\,0\,2\rangle$ cluster which occurs most frequently, while the results of [5, 6] practically exclude its existence. In the authors' opinion this difference can be explained by differences between the values of the components of the concentration expansion tensor used.

An analysis of the sequence of the co-ordination shells appearing in Table II, at decreasing V_{ij} potential values, reveals that the interactions extend over very large distances in some crystallographic directions, such as the *a*, *b* and *c* axes (five to six lattice constants), while in other directions, such as [1 1 1], the extent is relatively small. The above observation may be important in interpreting the process of forming large clusters.

3. Many-particle potentials

Like two-particle potentials, many-particle potentials determine the population of the corresponding many-particle clusters. Two factors affect the values of many-particle potentials. One of these is many-particle irreducible $V_{ij\ldots k}$ potentials, appearing in Hamiltonian Equation 1, and reducible potentials of the same order formed from appropriate combinations of irreducible potentials of lower orders. The reason for the presence of the latter is a non-linear relation between the internal energy and the Hamiltonian.

The diagram technique, developed for the Ising model [22], and adopted for two-component alloys [23], makes it possible to calculate reducible many-particle potentials of arbitrary order. This gives good results in the application to substitutional alloys [24]. It cannot be applied, however, to the system considered here, since it is based on high temperature expansions satisfying condition $V_{ij\ldots k}/kT < 1$. As it follows from Table II, the calculated potential values satisfy the exactly opposite relation at 300 K ($kT = 0.025\,85$ eV). In [7], an expansion of internal energy into a series convergent at low temperatures was proposed, but analysis of the system, with the presence of large clusters in mind, performed by this method is extremely cumbersome. In the present paper another approach is proposed.

Let one consider a partition function of the Gibbs' ensemble, which in the notation of Equation 1 has the form

$$Z = \exp\left(-\frac{1}{2kT}\sum_{ij} V_{ij}\hat{C}_i\hat{C}_j + \cdots - \frac{1}{n!kT}\sum_{ij\ldots k} V_{ij\ldots k}\hat{C}_i\hat{C}_{j\ldots k}\hat{C}_k\right) \quad (5)$$

For a specified three-particle cluster of fixed suffixes, *i*, *j* and *k*, the factor representing this cluster in the partition function is as follows

$$Z_{ijk} = \exp[-(V_{ij}\hat{C}_i\hat{C}_j + V_{jk}\hat{C}_j\hat{C}_k + V_{ik}\hat{C}_i\hat{C}_k + V_{ijk}\hat{C}_i\hat{C}_j\hat{C}_k)/kT] \quad (6)$$

If all sites *i*, *j* and *k* are occupied ($\hat{C}_i = \hat{C}_j = \hat{C}_k = 1$), equation 6 is equivalent to

$$Z_{ijk} = \exp(-V'_{ijk}\hat{C}_i\hat{C}_j\hat{C}_k/kT) \quad (7)$$

where

$$V'_{ijk} = V_{ij} + V_{jk} + V_{ik} + V_{ijk}.$$

Thus, the total equivalent potential in a three-particle cluster is equal to the sum of the potentials of all two-particle interactions, plus potential V_{ijk} accounting for a change of two-particle potentials as a result of the presence of the third atom. An identical result holds for a cluster of arbitrary size; it is necessary to sum possible interaction potentials of the highest possible order and of all other lower orders. Accounting for Equation 7 partition Equation 5 is presented in the form

$$Z = Z_{ij} \times Z_{ijk} \times \cdots Z_{ij\ldots k} \times \cdots \quad (8)$$

where Z_{ij}, $Z_{ijk}, \ldots, Z_{ij\ldots k}$, represent the contributions of successive two-, three-, ..., *n*-particle clusters. By replacing all these factors with their thermodynamic mean values, and after a routine procedure one can obtain an expression for the internal energy

$$U = \frac{1}{2}\sum_{ij}{}' V'_{ij}\langle\hat{C}_i\hat{C}_j\rangle + \frac{1}{3!}\sum_{ijk}{}' V'_{ijk}\langle\hat{C}_i\hat{C}_i\hat{C}_k\rangle + \cdots + \frac{1}{n!}\sum_{ij\ldots k}{}' V'_{ij\ldots k}\langle\hat{C}_i\hat{C}_j\ldots\hat{C}_k\rangle + \cdots \quad (9)$$

where symbol Σ' means that in each such sum, all lattice sites taking part in the formation of the clusters of other orders are excluded. As a matter of fact, Equation 9 represents an expansion of internal energy over the contributions of corresponding clusters and this way of grouping is typical for cluster methods. In Equation 9 all total multiparticle potentials, $V'_{ij\ldots k}$ are temperature independent. This is a result of low temperature approximation and, in particular, of neglecting fluctuations of factors $Z_{ij\ldots k}$. For comparison, when the internal energy is calculated in super high temperature approximation, the contributions of all diagrams giving rise to the presence of reducible interaction potentials vanish and only irreducible potentials remain in $V'_{ij\ldots k}$.

At absolute zero, Equation 9 is simplified in a natural way, since all clusters except that with the lowest binding energy disappear. If there are *n* atoms in such a cluster, the total number of clusters in $N\,C/n$, where *N* is the total number of lattice sites and *C* the atomic concentration of impurity, i.e.

$$U = NCV'_{ij\ldots k}/n \quad (10)$$

As it may be seen from Equation 10, the cluster with the smallest binding energy per atom (this energy has a negative sign) is the most favourable energetically. In such a case, only this factor, associated with a unique configuration, participates in the partition function, Equation 8. It is identical in all components to the partition function. It follows that Equation 10 is accurate at 0 K.

As the temperature rises these clusters decay and other clusters appear with less favourable binding energy, and Equation 10 gradually converts into Equation 9. Let one consider this process in more detail.

For the sake of simplicity of further considerations, order the clusters in succession of growing binding energy, i.e. in the order of decreasing population of clusters. Equation 9 can be written in the form

$$U = N\sum_{\alpha} V_\alpha C_\alpha \tag{11}$$

where V_α equals $V'_{ij\ldots k}/n_\alpha$; n_α is the number of atoms in cluster number α; C_α is the probability that a given atom belongs to cluster α.

Now, calculate the entropy of the system by the combination method. It is easy to calculate that the total number of clusters of type α in NC_α/n_α. Then, calculate the total number of sites in the crystal, allowed by the given crystallographic structure, possible to be occupied by such a cluster. By translating a given cluster over the whole crystal one obtains N such possibilities. Moreover, at a fixed site, there are R_α possibilities of rotations transforming a given cluster into another one, equivalent crystallographically. In the case of two-particle clusters, R_α is a well known co-ordination number. In effect, one can obtain NR_α possibilities. If the cluster is of two-particle type, e.g. with lattice sites r_1 and r_2, this cluster twice can be counted; once when $r_i = r_1$, and the second time when $r_i = r_2$. By analogy, the three-particle clusters will be counted three times, and in general n-particle clusters will be counted n times. As a final result, a given cluster configuration can be accomplished in the crystal in NR_α/n_α ways. The above result makes it possible to calculate the entropy of each atom bound in an arbitrary cluster. Omitting technical details of calculations, the total configuration entropy of the system can be written as

$$S = -kN\sum_{\alpha}\{R_\alpha \ln(1 - C_\alpha/R_\alpha) + C_\alpha \ln[C_\alpha/(R_\alpha - C_\alpha)]\} \tag{12}$$

Treating parameters C_α as variation parameters, from the condition of the minimum of free energy, $F = U - TS$, one obtains after differentiation, the equilibrium values of these parameters

$$C_\alpha/(R_\alpha - C_\alpha) = N_0 \exp[-V_\alpha/kT] \tag{13}$$

Normalization constant N_0 appears in Equation 13 as a result of taking into account the law of conservation of the total number of particles in the system, which in this notation can be written as

$$\sum_{\alpha} C_\alpha = C \tag{14}$$

The value of this constant can be found numerically by substituting the actual value of atomic concentration, C, into Equation 14. If condition $R_\alpha \gg C$ is satisfied, which is usually the case since $R_\alpha \geqslant 1$, then approximately

$$N_0 = C/\sum_{\alpha} R_\alpha \exp(-V_\alpha/kT) \tag{15}$$

In this approximation, another approximate relation based on Equation 15 is valid

$$C_\alpha/C_\beta = R_\alpha \exp[(-V_\alpha + V_\beta)/kT]/R_\beta \tag{16}$$

In view of the adopted assumptions (ignoring fluctuations of factors ΔZ_{ij} in partition Equation 8) the obtained solution is approximate and can be used at low temperatures. The actual expressions for C_α make it possible to estimate the temperature range of the applicability of the obtained solutions, the necessary condition being $-V_\alpha/kT \gg 1$, at least for one type of cluster. For carbon martensite, in view of the values of two-particle potentials listed in Table II for $\langle 0\,0\,2\rangle$ co-ordination, the value of this ratio at 500 K amounts to 8.36; whereas for five-particle clusters, as shall be demonstrated below, this value amounts to 12.2 at 500 K. Summarizing, in the case of carbon martensite the proposed method can be used practically over the whole temperature range of the existence of this phase.

The proposed method is closely related to high and medium temperature solutions used previously in [7, 8, 24], but transformed to the range of super low temperatures. As a result, by adopting the basic solution at absolute zero, the problem has been reduced to the original cluster method.

The presently used cluster methods have been developed mostly in order to solve problems typical of magnetic clusters, by taking into account the quantum nature of the object and adopting the appropriate mathematical tools [25, 26]. In such form they are difficult to adapt to the problems of atomic ordering.

The approach given here, in view of the simple form of the obtained solutions, is comparable to earlier cluster methods [27–30]. However, in comparison to these it remains sufficiently general. There are no *a priori* limitations concerning the range of interaction and the type and size of clusters. Moreover, the developed method does not refer directly to a particular crystalline structure. Accordingly, it can be easily applied to other interstitial alloys and to other types of crystallographic structure.

4. Multiparticle clusters in carbon martensite

Now, consider the populations of various carbon clusters in thermodynamic equilibrium conditions. As follows from Table II, this is cluster C–C $\langle 0\,0\,2\rangle$, which is the most favourable energetically among the two-particle clusters. This cluster is denoted by α_1 in Table III. The next one, cluster C–C $\frac{1}{2}\langle 1\,1\,1\rangle$ is denoted by α_2. In Table IV, mutual relations between the concentrations of carbon bound in the respective clusters at 78, 300 and 500 K are presented, calculated on the basis

TABLE III Clusters of IInd to Vth order with the highest binding energies per carbon atom. Columns 3–6 present lattice positions of atoms r_j–r_m, bound in a given cluster. Lattice positions are determined with respect to a carbon atom located at the 000 position in the O_c sublattice. Column 7 shows binding energy per atom in a given cluster.

Order	Symbol	r_j			r_k			r_l			r_m			V_α (eV)
I	2	3			4			5			6			7
II	α_1	0	0	2		–			–			–		– 0.360
	α_2	1/2	1/2	1/2		–			–			–		– 0.184
III	β_1	0	0	2	0	0	– 2		–			–		– 0.466
	β_2	0	0	2	1/2	1/2	5/2		–			–		– 0.381
	β_3	1/2	1/2	1/2	1	0	0		–			–		– 0.311
IV	γ_1	0	0	2	0	0	– 2	0	0	4		–		– 0.503
	γ_2	1/2	1/2	1/2	$\bar{1}$/2	1/2	1/2	0	0	$\bar{2}$		–		– 0.441
	γ_3	1	0	2	0	0	2	1	0	0		–		– 0.402
	γ_4	1	0	0	0	0	$\bar{2}$	1/2	1/2	1/2		–		– 0.399
	γ_5	1	0	0	0	1	0	1/2	1/2	1/2		–		– 0.389
	γ_6	1	0	0	1/2	1/2	1/2	3/2	1/2	1/2		–		– 0.386
	γ_7	0	0	2	1/2	0	1	0	0	$\bar{2}$		–		– 0.377
	γ_8	1	0	2	0	0	2	0	0	$\bar{2}$		–		– 0.371
	γ_9	1/2	1/2	1/2	3/2	1/2	1/2	0	0	$\bar{2}$		–		– 0.338
V	δ_1	0	0	2	0	0	– 2	0	0	4	0	0	– 4	– 0.526
	δ_2	1	0	0	0	1	0	1	1	0	1/2	1/2	1/2	– 0.475
	δ_3	0	0	2	0	0	$\bar{2}$	1	0	2	1	0	0	– 0.435
	δ_4	0	0	2	0	0	$\bar{2}$	0	0	4	1/2	0	1	– 0.425

TABLE IV Mutual relations between carbon concentrations in clusters at various temperatures in thermodynamic equilibrium. The notation of clusters is as for Tables III and V.

C_i/C_j	Temperature (K) 78	300	500
C_{α_1}/C_{β_1}	2.83×10^{-7}	0.033	0.171
$C_{\alpha_1}/C_{\gamma_1}$	5.75×10^{-10}	3.96×10^{-3}	0.036
$C_{\alpha_1}/C_{\delta_1}$	1.88×10^{-11}	3.25×10^{-3}	0.042
$C_{\alpha_1}/C_{\Delta_6}$	1.22×10^{-14}	8.65×10^{-5}	2.10×10^{-3}
$C_{\alpha_1}/C_{\Delta_7}$	2.34×10^{-19}	5.14×10^{-6}	3.85×10^{-4}
$C_{\alpha_1}/C_{\Delta_8}$	3.11×10^{-23}	5.04×10^{-7}	9.57×10^{-5}
$C_{\alpha_1}/C_{\Delta_9}$	4.68×10^{-26}	2.60×10^{-7}	1.12×10^{-4}
$C_{\alpha_1}/C_{\Delta_{20}}$	4.11×10^{-41}	3.16×10^{-11}	5.01×10^{-7}
$C_{\alpha_1}/C_{\Delta_\infty}$	0	3.76×10^{-33}	3.51×10^{-20}
$C_{\alpha_2}/C_{\alpha_1}$	1.70×10^{-11}	4.42×10^{-3}	0.067
C_{β_2}/C_{β_1}	1.29×10^{-5}	0.149	0.556
C_{β_3}/C_{β_1}	9.42×10^{-10}	1.57×10^{-3}	0.126
$C_{\gamma_2}/C_{\gamma_1}$	3.94×10^{-5}	0.363	0.949
$C_{\gamma_3}/C_{\gamma_1}$	1.19×10^{-6}	0.080	0.384
$C_{\gamma_4}/C_{\gamma_1}$	7.62×10^{-7}	0.072	0.358
$C_{\gamma_5}/C_{\gamma_1}$	1.72×10^{-7}	0.049	0.284
$C_{\gamma_6}/C_{\gamma_1}$	1.10×10^{-7}	0.043	0.265
$C_{\gamma_7}/C_{\gamma_1}$	2.89×10^{-8}	0.031	0.215
$C_{\gamma_8}/C_{\gamma_1}$	1.18×10^{-8}	0.024	0.187
$C_{\gamma_9}/C_{\gamma_1}$	8.71×10^{-11}	6.76×10^{-3}	0.087
$C_{\delta_2}/C_{\delta_1}$	4.05×10^{-3}	1.11	2.45
$C_{\delta_3}/C_{\delta_1}$	1.05×10^{-5}	0.237	0.968
$C_{\delta_4}/C_{\delta_1}$	2.38×10^{-6}	0.161	0.767
$C_{\Gamma_6}/C_{\Delta_6}$	3.59×10^{-4}	0.046	0.090
$C_{\Gamma_7}/C_{\Delta_7}$	6.70×10^{-10}	2.36×10^{-3}	6.41×10^{-3}
$C_{\Gamma_8}/C_{\Delta_8}$	8.22×10^{-15}	9.35×10^{-5}	2.20×10^{-3}
$C_{\Gamma_9}/C_{\Delta_9}$	1.70×10^{-18}	1.20×10^{-5}	8.45×10^{-4}
$C_{\Delta_{20}}/C_{\Delta_\infty}$	4.72×10^{-85}	1.19×10^{-22}	7.00×10^{-14}

of Equation 16. The number of the presented data is sufficient to calculate others, not included in the table values for all considered clusters, using simple algebraic operations. As may be seen, the ratio of the carbon concentrations in clusters α_1 and α_2, $C_{\alpha_2}/C_{\alpha_1}$ amounts to 1.7×10^{-11} at 78 K and to 0.0044 at 300 K. The populations of other clusters in this temperature interval are negligibly small. In the class of three-particle clusters, using the above criteria, three clusters may be considered, denoted in Table III as β_1, β_2 and β_3, with configurations C–C⟨0 0 2⟩–C⟨0 0 $\bar{2}$⟩, C–C⟨0 0 2⟩–C$\frac{1}{2}$⟨1 1 5⟩ and C–C$\frac{1}{2}$⟨1 1 1⟩–C⟨1 0 0⟩. The ratios C_{β_2}/C_{β_1}, and C_{β_3}/C_{β_1} amount to 1.29×10^{-5} and 9.42×10^{-10}, respectively at 78 K and to 0.149 and 0.002, respectively, at 300 K.

Table III contains the values of V_α potentials for clusters of order II to V, which can be possibly taken into consideration in an analysis of short range order in martensite. It follows from the data presented in Table IV that in the group of all clusters, including five-particle ones, this is a five-particle linear cluster which should occur most frequently. In this cluster (denoted by δ_1 in Table III) the carbon atoms are located at octahedral vacant sites O_c along the tetragonal c axis, and are separated from each other by two lattice constants. The contributions of analogous four-atom clusters (without one of the extreme carbon atoms) denoted by γ_1 are also significant; the ratio $C_{\gamma_1}/C_{\delta_1}$ equals 0.033 and 0.82 at 78 and 300 K, respectively. The number of three-particle clusters of the same type, denoted by β_1 is small; the ratio C_{β_1}/C_{δ_1} amounts to 6.6×10^{-4} and 0.098 at 78 and 300 K, respectively. All two-particle clusters, even if they were formed at the initial stage of clusterization should practically vanish in the course of approaching thermodynamic equilibrium.

In the group of five-particle clusters, there appears a cluster denoted by δ_2 representing a pyramid with the base in the (0 0 1) plane. Its contribution $C_{\delta_2}/C_{\delta_1}$ amounts to 4.05×10^{-3} at 78 K, but it is already 1.11 at 300 K. By comparison, its four-particle counterpart, a pyramid with one unoccupied site at the base diagonal (denoted by γ_5) has a small population: the ratio $C_{\gamma_5}/C_{\delta_1}$ amounts to 2.4×10^{-9} and 0.04 at

78 and 300 K, respectively. The three-particle cluster mentioned in the introduction and observed in [4] is a fragment of clusters γ_5 and δ_2.

Clusterization does not need to terminate at five-particle clusters. In the next paragraph, the likelihood of the presence of larger clusters in the system is analysed.

5. Hypothetical presence of superstructure in martensite

It follows from the above discussion of the system that two five-particle clusters, types, δ_1 and δ_2, are present in martensite. These clusters can eventually grow into larger clusters or superstructures. Table V presents the most energetically favourable clusters from the VIth to IXth order, built on the basis of the above-mentioned five-particle δ_1 and δ_2 clusters. It follows from this table that the δ_1-based clusters have still less favourable binding energy than the initial δ_1 cluster, and are not competitive in comparison to other clusters of the same order. Therefore this cluster will not grow. An exactly opposite relation holds for cluster δ_2. The cluster denoted in Table V as Δ_9 and composed of nine carbon atoms will decisively dominate over the initial δ_2 and all remaining clusters.

As a next step, consider the possibility of aggregation of such clusters. The binding energy of two

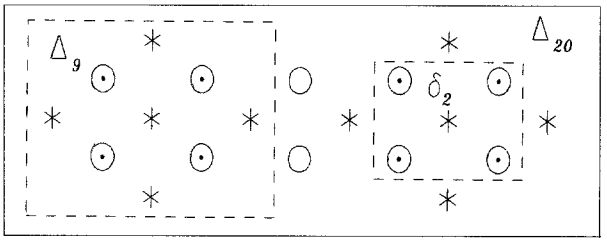

Figure 1 Twenty-particle cluster of Δ_{20} type O_c sublattice: (⊙) position of carbon atoms located in (0 0 1) plane: (*) projections of the positions of carbon atoms located in the parallel plane at a distance of 1/2 C lattice constant: and (○) positions of carbon atoms binding two Δ_9 clusters.

Δ_9 clusters is -1.376 eV. If, in addition, the two octahedral vacant sites between these clusters are filled (cf. Fig. 1), the binding energy increases by an additional -3.278 eV. In effect, the binding energy per atom in such 20-atom clusters, denoted as Δ_{20} in Table V amounts to a V_α of -0.985 eV. This is a much more favourable situation than that in cluster Δ_9. Like cluster Δ_9, cluster Δ_{20} can also grow. As the limit, the binding energy per carbon atom in an infinitely large cluster of this kind was calculated. In such a case, the calculations simplify since all atoms are equivalent (the boundary conditions disappear); and instead of summing the interactions of every atom with all others, it is sufficient to calculate one-half of the sum of interactions of a single atom with all others. As a result of such calculations, with 56 co-ordination shells taken into account, i.e. with all atoms in this cluster up to a distance of eight lattice constants, a value of V_α equal to -2.29 eV was obtained. With this value, the ratio $C_{\Delta_{20}}/C_{\Delta_9}$ (see Table IV) amounts to 1.2×10^{-22} at 300 K. This result grants the presence of such superstructure; provided, however, that the initial cluster, δ_2, with unfavourable binding energy has been formed during the transient formation phase. In such a situation even 20-atom clusters, Δ_{20}, not speaking of all the remaining, have too low energy to exist in measurable quantities. Thus, the cluster in the form of an atomic layer, of half a lattice constant thickness, filling all octahedral vacant sites, O_c in the (0 0 1) plane, should attain dimensions comparable with the size of a given grain. The analysis of the values of potentials (see Table II) leads to a conclusion that the next such layer can appear not nearer than at a distance of three lattice constants.

In summary, five-particle clusters of δ_2 type form seeds for growing larger clusters, which next transform into superstructure. Other clusters presented in Table III have no conditions to grow into configurations of more than five atoms.

6. Conclusions

As was pointed out in the introduction, martensite obtained in the process of quenching is far from

TABLE V Binding energy per one particle in higher order clusters formed on the basis of five-particle clusters. Lattice positions and their notation as in Table III. Columns 4–7 give lattice positions of atoms attached to the initial cluster.

	Symbol	Initial cluster	r_i			r_j			r_k			r_l			V (eV)
I	2	3	4			5			6			7			8
VI	Γ_6	δ_1	0	0	6		–			–			–		-0.522
	Δ_6	δ_2	3/2	1/2	1/2		–			–			–		-0.566
VII	Γ_7	δ_1	0	0	6	0	0	-6		–			–		-0.511
	Δ_7	δ_2	3/2	1/2	1/2	1/2	3/2	1/2		–			–		-0.639
VIII	Γ_8	δ_1	0	0	6	0	0	-6	0	0	8		–		-0.495
	Δ_8	δ_2	3/2	1/2	1/2	1/2	3/2	1/2	$\bar{1}/2$	1/2	1/2		–		-0.699
IX	Γ_9	δ_1	0	0	6	0	0	-6	0	0	8	0	0	-8	-0.477
	Δ_9	δ_2	3/2	1/2	1/2	1/2	3/2	1/2	$\bar{1}/2$	1/2	1/2	1/2	$\bar{1}/2$	1/2	-0.752
XX	Δ_{20}	$\Delta_9 + \Delta_9$	2	0	0	2	1	0		–			–		-0.985
∞	Δ_∞	Δ_{20}		–			–			–			–		-2.290

thermodynamic equilibrium. Such equilibrium is attained in the process of formation of appropriate multiparticle clusters. In view of the obtained results, the clusterization process may proceed in various ways, depending on the conditions. Consider the process of formation of low temperature clusters (at 78 K), under the assumption that the obtained martensite has anomalous tetragonality, i.e. only O_c positions are occupied. The carbon atoms, the majority of which one dispersed in an isolated form after quenching, will aggregate into larger and larger clusters; first primarily into α_1, β_1 and γ_1, and finally into δ_1 (cf. Table III). At elevated temperature, a reverse process will take place; larger clusters will disintegrate into smaller ones. This process is not associated with overcoming the potential barrier and is quasi-reversible. A different situation occurs in the case of clusters δ_2, which are the seeds for superstructures. At the considered temperature, their equilibrium population is low, i.e. about 0.4%. The population of other clusters of similar topology and lower order (γ_2, γ_3, see Table IV) is also low. Nevertheless, if these clusters are already formed, they will immediately grow to much larger sizes at the expense of their initial form. Since this disturbs thermodynamic equilibrium, new δ_2 clusters must be formed. Thus, if the system is allowed to stay at low temperature for a sufficiently long time a superstructure will be formed, the process being irreversible. In view of its high binding energy, the superstructure thus formed should exhibit significant thermal stability as regards ordering changes and order–disorder phase transitions, as well as other phase transformations, e.g. carbide formation.

The process should proceed faster at higher temperatures, e.g. at room temperature. However, there exists competitive processes which can transform the system into another local minimum of free energy. At higher temperatures a fraction of the atoms in the O_c sublattice will move to the O_a and O_b sublattices. With elapsing time, single, initially isolated, carbon atoms will form analogous clusters in these sublattices. Part of them can also participate in the formation of mixed clusters, O_c–O_a and O_c–O_b, such as γ_7 and δ_4. The formation of clusters in these sublattices will block the diffusion process and make migration of atoms from one sublattice to another an irreversible process.

The above results are based on harmonic approximation. In the author's opinion, verification of possible corrections introduced by accounting for irreducible higher order potentials should be accomplished in an experimental way.

Acknowledgements

The author is thankful to Professor J. Suwalski for his valuable comments and suggestions. This work was sponsored by the KBN Research Programme.

References

1. V. V. SUMIN, M. G. ZEMLIANOV, L. M. KAPUTKINA, P. P. PARSHIN, C. D. PROKOSHKIN and A. I. TCHOKLO, *Fiz. Met. Metalloved. (USSR)* **11** (1992) 122.
2. I. R. ENTIN, V. A. SOMENKOV and S. S. SHILSTEIN, *Dokl. Akad. Nauk USSR* **206** (1972) 1096.
3. R. A. JOHNSON, *Acta Metall.* **13** (1965) 1259.
4. J. M. R. GENIN, *Metall. Trans. A* **18A** (1987) 1371.
5. G. V. KURDIUMOV and A. G. KHACHATURYAN, *Acta Metall* **23** (1975) 1077.
6. M. S. BLANTER and A. G. KHACHATURYAN, *Metall Trans. A* **9A** (1978) 753.
7. L. DABROWSKI, *J. Mater. Sci.* **25** (1990) 2722.
8. Idem, *J. Magn. Magn. Mater.* **81** (1989) 173.
9. A. G. KHACHATURYAN, *Fiz. Tverd. Tela (USSR)* **9** (1967) 2861.
10. H. E. COOK and D. DE FONTAINE, *Acta Metall.* **17** (1969) 915.
11. *Idem, ibid.* **19** (1971) 607.
12. D. W. HOFFMAN, *ibid.* **18** (1970) 819.
13. A. G. KHACHATURYAN, "Theory of Structural Transformation in Solids" (Wiley, New York, 1983), and also in "Nauka", (Moscow, 1974) p. 322.
14. V. J. MINKIEWICZ, G. SHIRANE and R. NATHANS, *Phys. Rev.* **162** (1967) 528.
15. B. N. BROCKHOUSE, H. E. ABOU-HELAL and E. D. HALLMAN, *Solid State Commun* **5** (1967) 211.
16. C. VAN DIJK and J. BERGSMA, *Neutron Inelastic Scattering* **1** (1968) 233.
17. A. D. B. WOODS, "Inelastic Scattering of Neutron in Solids and Liquids", Vol. II (International Atomic Eng. Agency, Vienna, 1963) p. 3.
18. O. ANTSON, V. G. GAVRILYUK, V. A. KUDRIASHOV, V. M. NADUTOV, K. PEYURYU, Y. PETIKAYNEN, A. TITTA, V. A. TRUDNOV, K. ULLAKKO, V. A. ULIANOV, P KHIISMYAKI and Y. P. THERNENKOV, *Fiz. Met. Metalloved. (USSR)* **10** (1990) 114.
19. M. HAYAKAWA and M. TANIGAMI, *M. Oka, Met. Trans. A* **16A** (1985) 1745.
20. L. DABROWSKI, J. SUWALSKI, V. CHRISTOV, B. SIDZHIMOV and P. MAŁECKI, Report IAE-2144/VIII Otwock-Swierk (1993).
21. J. A. RAYNA and B. S. CHANDRASEKHLER, *Phys. Rev.* **122** (1961) 1714.
22. G. HORVITZ and H. CALLEN, *ibid.* **124** (1961) 1757.
23. D. A. BADALYAN and A. G. KHACHATURYAN, *Fiz. Tverd. Tela (USSR)* **12** (1970) 439.
24. L. DABROWSKI, *Phys. Status Solidi* **128B** (1985) 371.
25. J. W. TUCKER, *J. Appl. Phys.* **69** (1991) 6164.
26. W. METZNER, *Phys. Rev. B* **43** (1991) 8549.
27. R. KIKUCHI, *Phys. Rev.* **81** (1951) 988.
28. *Idem, J. Chem. Phys.* **19** (1951) 1230.
29. N. S. GOLOSOV, L. E. POPOV and L. Y. PUDAN, *J. Phys. Chem. Solids* **34** (1973) 1149.
30. *Idem, ibid.* **34** (1973) 1157.

Received 2 February
and accepted 6 July 1994